

Evidence that the AT transition disappears below six dimensions

Bharadwaj Vedula,¹ M. A. Moore,² and Auditya Sharma¹

¹*Department of Physics, Indian Institute of Science Education and Research, Bhopal, Madhya Pradesh 462066, India*

²*Department of Physics and Astronomy, University of Manchester, Manchester M13 9PL, United Kingdom*

(Dated: March 29, 2024)

One of the key predictions of Parisi's broken replica symmetry theory of spin glasses is the existence of a phase transition in an applied field to a state with broken replica symmetry. This transition takes place at the de Almeida-Thouless (AT) line in the $h - T$ plane. We have studied this line in the power-law diluted Heisenberg spin glass in which the probability that two spins separated by a distance r interact with each other falls as $1/r^{2\sigma}$. In the presence of a random vector-field of variance h_r^2 the phase transition is in the universality class of the Ising spin glass in a field. Tuning σ is equivalent to changing the dimension d of the short-range system, with the relation being $d = 2/(2\sigma - 1)$ for $\sigma < 2/3$. We have found by numerical simulations that $h_{\text{AT}}^2 \sim (2/3 - \sigma)$ implying that the AT line does not exist below 6 dimensions and that the Parisi scheme is not appropriate for spin glasses in three dimensions.

I. INTRODUCTION

The relevance of the replica symmetry breaking (RSB) scheme of Parisi [1, 2] for physical spin glasses in three dimensions has occasioned doubts from its earliest days [3]. These doubts have mostly arisen from studies of the de Almeida-Thouless (AT) line [4]. This is the line in the field h and temperature T plane where the replica symmetric high-temperature phase changes to a phase with broken replica symmetry (see Fig. 1). The Parisi scheme has now been rigorously proved to solve the Sherrington-Kirkpatrick (SK) mean-field model [5], in which all spins interact with each other. In that model in the presence of a field h , the AT line $h_{\text{AT}}(T)$ for temperatures T close to T_c , the zero-field transition temperature, takes the form

$$\left(\frac{h_{\text{AT}}(T)}{T_c}\right)^2 = A(d) \left(1 - \frac{T}{T_c}\right)^\zeta. \quad (1)$$

The exponent $\zeta = 3$ in the SK model and remains at 3 for all $d > 8$. It takes the value $d/2 - 1$ when $8 > d > 6$ [6, 7]. For $d < 6$, should the AT line then still exist, $\zeta = \gamma + \beta$, where the exponent γ describes the divergence of the zero-field spin glass susceptibility χ_{SG} as $T \rightarrow T_c$, and β describes how the Edwards-Anderson order parameter q_{EA} goes to zero in the same limit [7]. Both these zero-field exponents have an expansion in powers of ϵ where $d = 6 - \epsilon$ [8]. Back in 1980 Bray and Roberts [3] were unable to find a fixed point for the exponents at the AT line. One possibility which they suggested as an explanation was that for $d < 6$ there simply was no AT line. However, the possibility that there was a non-perturbative fixed point could not be ruled out (but if such exists, it still remains to be discovered).

Another argument suggested long ago was that of Moore and Bray [10]. In $d < 6$ the dependence on γ and β of the form of the AT line as $\zeta = \gamma + \beta$ indicates that the applied field h has the scaling dimension of the ordering field of the spin glass. For $d > 6$ that is not the case, as then $\gamma + \beta = 2$ for all $d > 6$. Usually when the ordering field is present there is no phase transition. For

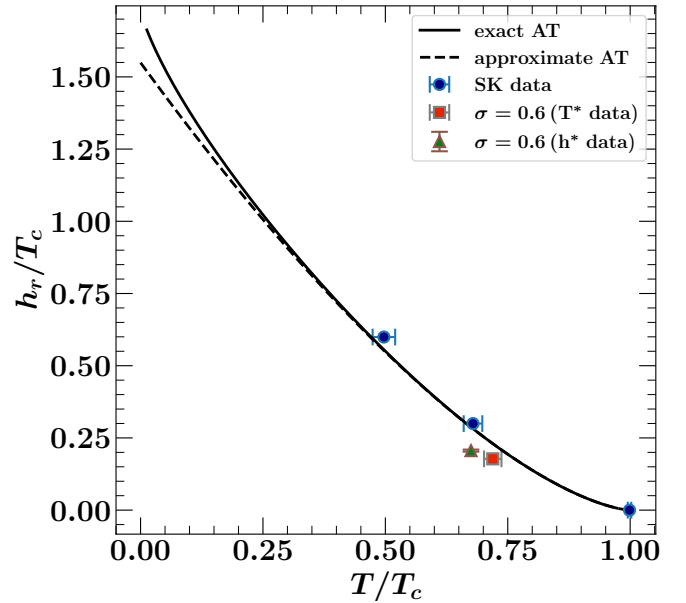


FIG. 1. The AT line. The solid line is the exact AT line for the SK model, calculated as in Ref. [9]. The dashed line is the approximation to it of Eq. (1) with $\zeta = 3$. Marked on the diagram by filled circles are the results of the simulations on the SK model in Ref. [9]. The red square point, derived from varying the temperature T at fixed h_r , and the upwards arrow point, derived from varying the field at fixed temperature, are the result of our simulations at $\sigma = 0.6$, which despite corresponding to 10 dimensions, have values of h_{AT} suppressed by fluctuations from those which would be estimated from the SK model when only adjusting the zero-field transition temperature T_c .

example, for a ferromagnet in its ordering field (which is a uniform field) there is no phase transition as the temperature is lowered. A phase transition only occurs for vanishing field. The suggestion of Moore and Bray was that because the applied field had the scaling dimensions of the ordering field in dimensions $d < 6$ then there would also be no phase transition in a field and hence no AT

line when $d < 6$ [10]. Even though it is commonplace that a phase transition is removed in the presence of the ordering field, alternatives are possible and some were discussed in Ref. [11], but no evidence for them was found.

Another argument that 6 might be the dimension above which RSB applies comes from RSB calculations of the interface free energy of the Ising spin glass in the presence of no external field. The calculations which are valid for $d > 6$ are done for a system of length L in one direction and M in the other $d - 1$ directions. The interface free energy ΔF is the change in the free energy when the boundary conditions in the L direction are switched from periodic to anti-periodic [12, 13]. Its bond-average variance ΔF^2 is found to be of the form [13]

$$\Delta F^2 \sim N^{1/3} + L^2 f(L/M), \quad (2)$$

where $N = LM^{d-1}$. The leading term $\sim N^{1/3}$ is of an unusual form for an interface free energy as it only depends on the volume or number of spins in the system, and is of this form because interfaces according to RSB are space filling as their fractal dimension $d_s = d$. The second term is of the conventional aspect ratio scaling form which involves the ratio of L/M usually associated with interfaces whose fractal dimensions d_s are less than d and which are not space filling [14, 15]. Using a simple (and approximate) renormalization group procedure it has been found that $d_s \rightarrow d$ as $d \rightarrow 6$ from below [16]. The term $L^2 f(L/M)$ becomes $L^{2\theta} f(L/M)$ for $d < 6$, and then the first term will not be present. θ is the interface free energy exponent [14]. According to the numerical study of Boettcher [17] $\theta = 1.1(1)$ in six dimensions, which suggests it might be exactly 1 when $d = 6$. But the crucial point is that for $d > 6$ the first term dominates, but the second term becomes just as large as the first term right in $d = 6$ for $L \sim M$. This suggests that $d = 6$ is at least an important dimension for RSB in spin glasses and possibly its lower critical dimension, the dimension below which full replica symmetry breaking of the Parisi type is no longer to be found.

Interface free energies are determined by the nature of the zero-temperature fixed point of the system and its associated exponents such as θ . These exponents should be distinguished from those associated with the critical fixed point. The study of Bray and Roberts [3] was an expansion about the upper critical dimension of the AT line, which was taken to be 6. The argument of this paper that there is no RSB for $d \leq 6$, which if valid implies that the upper and lower critical dimensions for RSB behavior are both the same and equal to 6 – a most unusual situation!

If the lower critical dimension for the existence of the AT line is six, then one would expect that the AT line will become closer to the temperature axis as $d \rightarrow 6$. To see whether this is the case requires determination of the coefficient $A(d)$, but this is very challenging. In the SK limit for unit length m -component vector spins, $A(d) = 4m/(m+2)$: For the Heisenberg model studied in

this paper $m = 3$. By using an expansion in $1/m$, Moore argued that as $d \rightarrow 6$ from above $A(d) \sim (d-6)$ [18]. The numerical studies reported in this paper are consistent with this possibility. They indeed imply therefore that the AT line is approaching the temperature axis as $d \rightarrow 6$, and hence that there will not be an AT transition below six dimensions.

The question of whether there is or is not an AT line in physical dimensions such as $d = 3$ has naturally been studied by both experiment and by simulations. On the experimental side a negative answer was suggested by the work in Ref. [19], while a positive answer was provided in Ref. [20]. No consensus is found in simulations either: for a recent review see [21].

Because it is hard to do simulations above 6 dimensions (although recently an attempt was made to study the AT line in 6 dimensions [22]), we have done simulations on the one-dimensional proxy model where systems of large linear extent L can be studied. In Ref. [22] where a six-dimensional version was directly simulated, L was less than 8, but we can study values of L up to 65536.

We organised the paper into the following sections. In Sec. II we describe the model we used in detail. The quantities we studied and their finite size scaling forms near the AT transition point are given in Sec. III. In Sec. IV we show the results obtained by performing finite size scaling analyses on the data for five values of σ in the mean-field regime: 0.600, 0.630, 0.640, 0.650, and 0.655. In Sec. V, we show our analysis of $A(\sigma)$ versus σ which provided us strong evidence that the AT line disappears below $\sigma_c = 2/3$. In an earlier investigation on the XY model [23] we had studied it for σ values 0.60, 0.70, 0.75 and 0.85, and had observed that because the leading correction to scaling exponent ω approaches 0 as $\sigma \rightarrow \sigma_c = 2/3$ that it would be very challenging to determine whether the AT line goes away precisely at $\sigma = 2/3$. This means that as $\sigma \rightarrow 2/3$ one needs to go to ever larger values of the system size N to maintain the same level of accuracy. The largest value of σ which we studied, 0.655, is off the curve set by the next three smaller values and we think that is because for it the largest N values we could study were just too small for a reliable value of the AT field. Finally in Sec. VI we summarize our conclusions.

II. MODEL HAMILTONIAN

The Hamiltonian of our system is

$$\mathcal{H} = - \sum_{\langle i,j \rangle} J_{ij} \mathbf{S}_i \cdot \mathbf{S}_j - \sum_i \mathbf{h}_i \cdot \mathbf{S}_i, \quad (3)$$

where \mathbf{S}_i , a unit vector of $m = 3$ components, is a spin sitting on the i^{th} lattice site ($i = 1, 2, \dots, N$). The N ($\equiv L$) lattice sites are arranged around a ring of circumference N . So the distance between the spins at sites i and j [26]

$$r_{ij} = \frac{N}{\pi} \sin \left(\frac{\pi}{N} |i - j| \right), \quad (4)$$

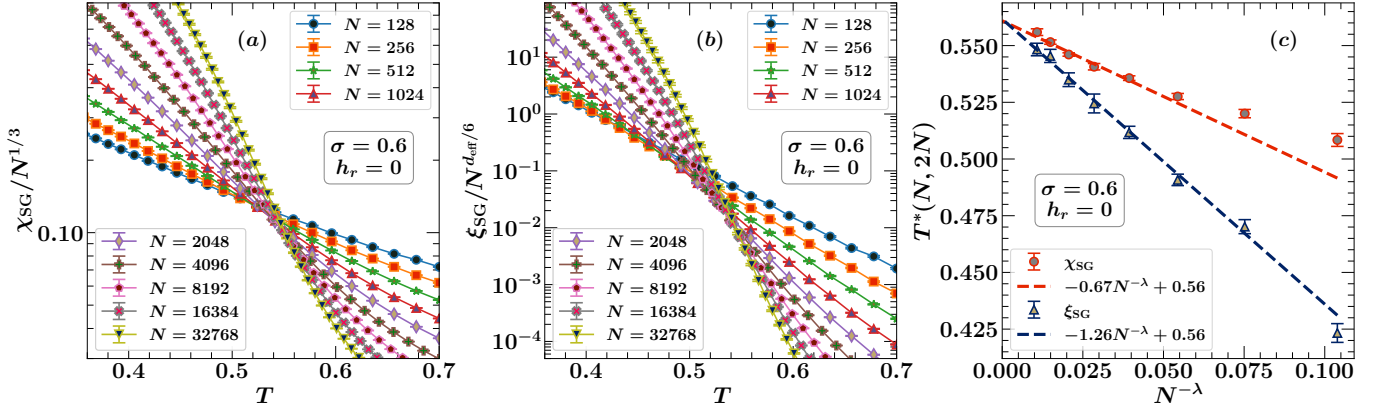


FIG. 2. Finite size scaling analyses of data for $\sigma = 0.600$ obtained by varying the temperature in the absence of a magnetic field. (a) shows the plot of $\chi_{\text{SG}}/N^{1/3}$ as a function of the temperature T for different system sizes. The corresponding data for $\xi_{\text{SG}}/N^{d_{\text{eff}}/6}$ are shown in (b), with $d_{\text{eff}} = 2/(2\sigma - 1)$ in the mean-field regime. Both the sets of plots show that the curves for different system sizes intersect. The data for the intersection temperatures $T^*(N, 2N)$ between pairs of adjacent system sizes for $\chi_{\text{SG}}/N^{1/3}$ and $\xi_{\text{SG}}/N^{d_{\text{eff}}/6}$ are plotted as a function of $N^{-\lambda}$ in (c). The value of the exponent λ is fixed to be 0.467 which is known exactly in the mean-field regime [24, 25]. The fits give $T_c = 0.5609 \pm 0.0012$ from χ_{SG} and $T_c = 0.5617 \pm 0.0021$ from ξ_{SG} (see Table I for details).

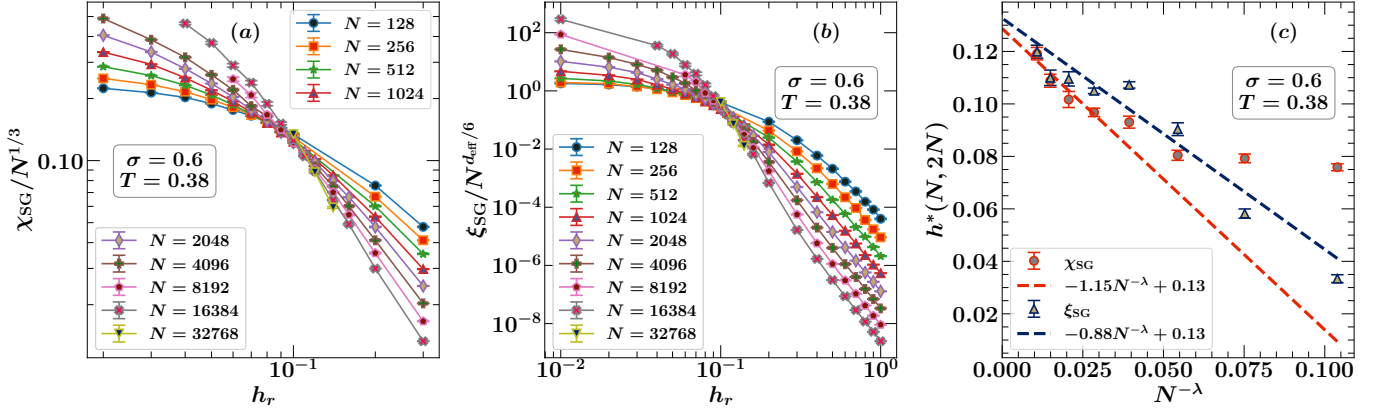


FIG. 3. Finite size scaling analyses of (a) χ_{SG} data, and (b) ξ_{SG} data, for $\sigma = 0.600$ obtained by fixing the temperature to $T = 0.380 (= 0.675 T_c)$ and varying the field. Both the plots show that the curves for different system sizes intersect. (c) shows the data for the intersection fields $h^*(N, 2N)$ between pairs of adjacent system sizes, plotted as a function of $N^{-\lambda}$. Using $\lambda = 0.467$ we fitted the $h^*(N, 2N)$ data linearly with Eq. (14) and the values of the transition field so obtained are $h_{\text{AT}}(T = 0.380) = 0.1287 \pm 0.0033$ from χ_{SG} and $h_{\text{AT}}(T = 0.380) = 0.1327 \pm 0.0015$ from ξ_{SG} (see Table II for details).

is the length of the chord connecting them. The probability of having a non-zero interaction between a pair of spins (i, j) falls with the distance r_{ij} between the spins as a power law:

$$p_{ij} = \frac{r_{ij}^{-2\sigma}}{\sum_{j \neq i} r_{ij}^{-2\sigma}}. \quad (5)$$

The interactions J_{ij} between a pair of spins (i, j) are independent Gaussian random variables with mean zero and standard deviation unity, i.e:

$$[J_{ij}]_{\text{av}} = 0 \quad \text{and} \quad [J_{ij}^2]_{\text{av}} = J^2 = 1. \quad (6)$$

The Cartesian components h_i^μ of the on-site external field are independent random variables drawn from a Gaussian

distribution of zero mean with each component having variance h_r^2 . The detailed prescription to generate such a lattice with long-range diluted interactions is given in references [23, 24, 27].

This model has already been extensively studied. Even though it involves spins of $m (= 3)$ components, its AT transition is in the universality class of the Ising ($m = 1$) model [9]. Despite the additional degrees of freedom of the spins compared to those of the Ising model, the Heisenberg model is easier to simulate than the Ising model as the vector spins provide a means to go around barriers rather than over them as in the Ising case, allowing larger systems to be simulated [28]. In the interval $1/2 < \sigma < 2/3$, it corresponds to an Edwards-Anderson

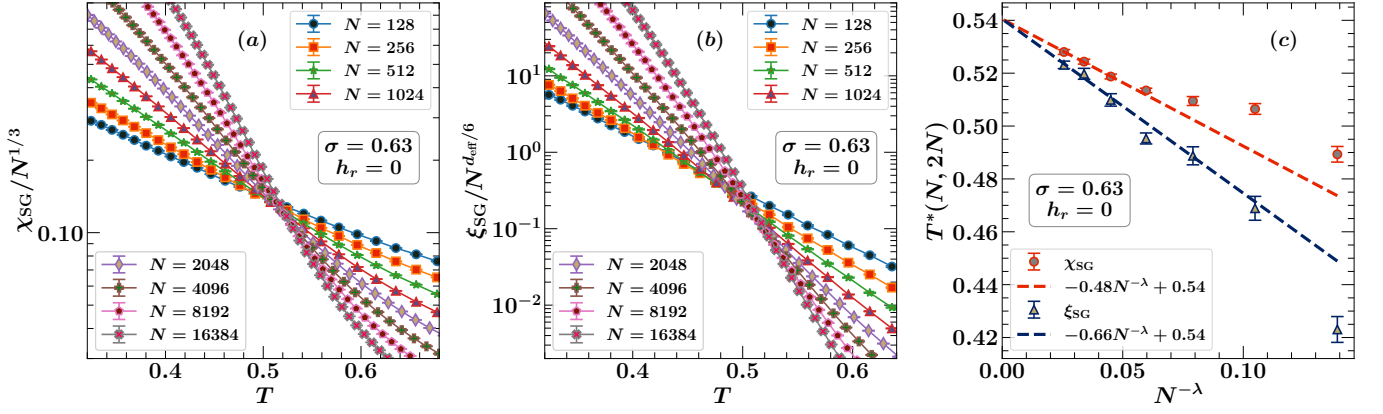


FIG. 4. Finite size scaling analyses of data for $\sigma = 0.630$ obtained by varying the temperature in the absence of a magnetic field. (a) shows the plot of $\chi_{\text{SG}}/N^{1/3}$ as a function of the temperature T for different system sizes. The corresponding data for $\xi_{\text{SG}}/N^{d_{\text{eff}}/6}$ are shown in (b), with $d_{\text{eff}} = 2/(2\sigma - 1)$ in the mean-field regime. Both the sets of plots show that the curves for different system sizes intersect. The data for the intersection temperatures $T^*(N, 2N)$ between pairs of adjacent system sizes for $\chi_{\text{SG}}/N^{1/3}$ and $\xi_{\text{SG}}/N^{d_{\text{eff}}/6}$ are plotted as a function of $N^{-\lambda}$ in (c). The value of the exponent λ is fixed to be 0.407 which is known exactly in the mean-field regime [24, 25]. The fits give $T_c = 0.5405 \pm 0.0024$ from χ_{SG} and $T_c = 0.5405 \pm 0.0045$ from ξ_{SG} (see Table I for details).

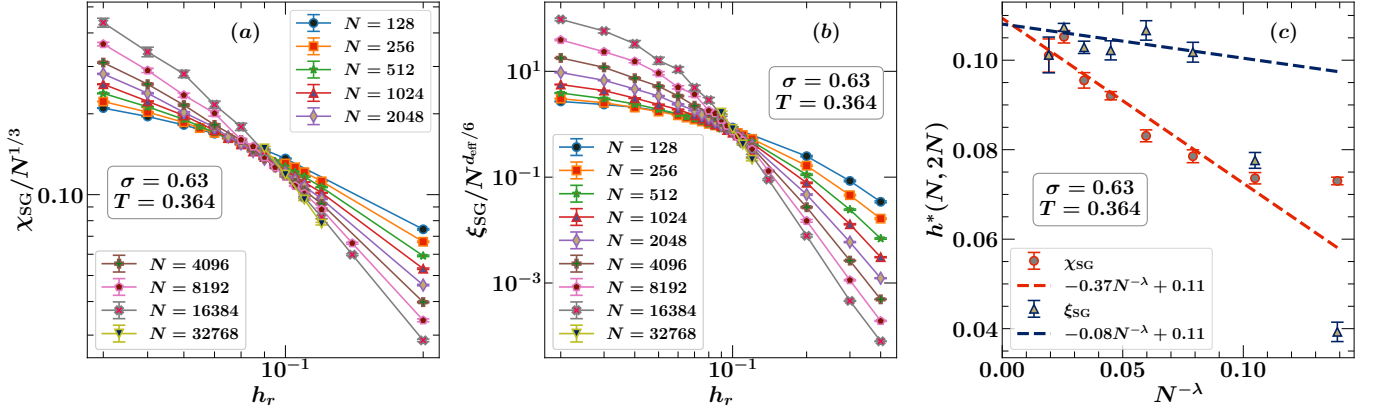


FIG. 5. Finite size scaling analyses of (a) χ_{SG} data, and (b) ξ_{SG} data, for $\sigma = 0.630$ obtained by fixing the temperature to $T = 0.364 (= 0.675 T_c)$ and varying the field. (c) shows the data for the intersection fields $h^*(N, 2N)$ plotted as a function of $N^{-\lambda}$. Using $\lambda = 0.407$ we fitted the $h^*(N, 2N)$ data linearly with Eq. (14) and the values of the transition field so obtained are $h_{\text{AT}}(T = 0.364) = 0.1094 \pm 0.0012$ from χ_{SG} and $h_{\text{AT}}(T = 0.364) = 0.1081 \pm 0.0015$ from ξ_{SG} (see Table II for details).

short-range model in d_{eff} dimensions [26], where

$$d_{\text{eff}} = \frac{2}{2\sigma - 1}. \quad (7)$$

Thus if $\sigma = 0.6$ (see Fig. 1), $d_{\text{eff}} = 10$. We ourselves have extensively studied the XY ($m = 2$) version of it [23], when we concentrated mainly on cases where $\sigma > 2/3$. Since writing that paper we have discovered that the Heisenberg case ($m = 3$) runs faster, enabling us to study larger systems. In this paper we have focussed on cases $\sigma < 2/3$ corresponding to $d > 6$ in an attempt to determine whether the AT line vanishes as $d \rightarrow 6$. At the time of writing of our paper on the XY spin glass model, we thought determining whether the AT line vanished as $\sigma \rightarrow 2/3$ would be very challenging as the corrections to scaling become larger and larger in

this limit, requiring the study of increasingly larger values of N to achieve the equivalent level of accuracy. Our work in this paper is indeed affected by this difficulty which prevents us getting really close to $\sigma = 2/3$ but it does suggest that the AT line might vanish at $d = 6$ (i.e. $\sigma = 2/3$) if the limit $N \rightarrow \infty$ could be studied.

III. CORRELATION LENGTHS AND SUSCEPTIBILITIES

As in the XY case we shall focus on the wave-vector-dependent spin glass susceptibility [24]

$$\chi_{\text{SG}}(k) = \frac{1}{N} \sum_{i,j} \frac{1}{m} \sum_{\mu,\nu} \left[(\chi_{ij}^{\mu\nu})^2 \right]_{\text{av}} e^{ik(i-j)}, \quad (8)$$

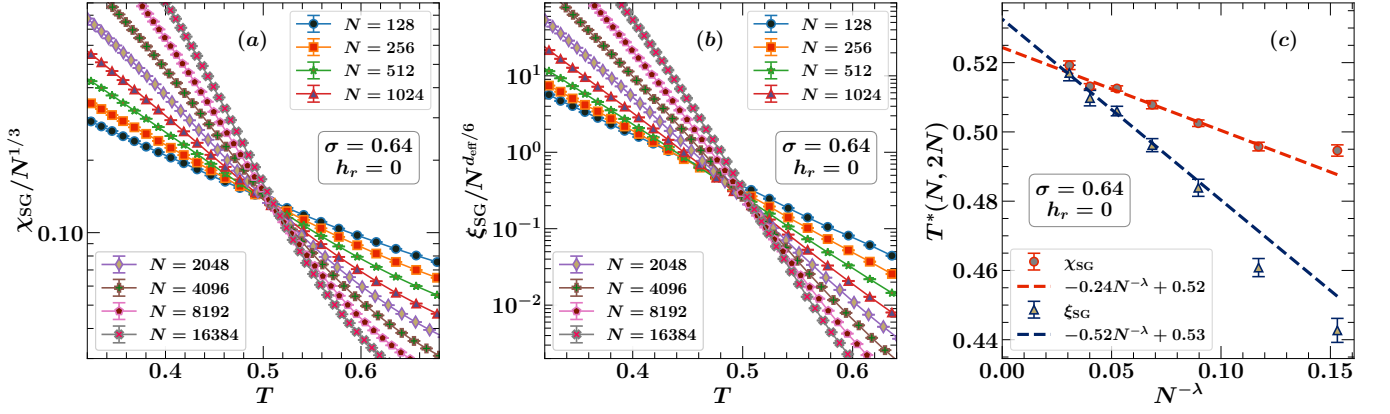


FIG. 6. Finite size scaling analyses of (a) χ_{SG} data, and (b) ξ_{SG} data, for $\sigma = 0.640$ obtained by varying the temperature in the absence of a magnetic field. (c) shows the data for the intersection temperatures $T^*(N, 2N)$ plotted as a function of $N^{-\lambda}$ with $\lambda = 0.387$. The line fits give $T_c = 0.5244 \pm 0.0020$ from χ_{SG} and $T_c = 0.5326 \pm 0.0038$ from ξ_{SG} (see Table I for details).

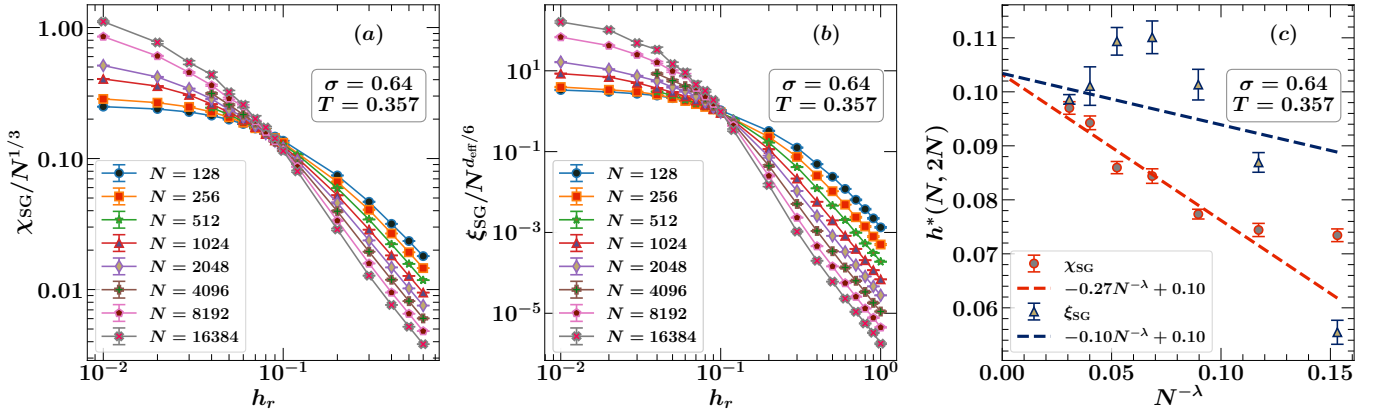


FIG. 7. Finite size scaling analyses of (a) χ_{SG} data, and (b) ξ_{SG} data, for $\sigma = 0.640$ obtained by fixing the temperature to $T = 0.357 (= 0.675 T_c)$ and varying the field. (c) shows the data for the intersection fields $h^*(N, 2N)$ between pairs of adjacent system sizes, fitted against $N^{-\lambda}$, using $\lambda = 0.387$. The values of the transition field so obtained are $h_{\text{AT}}(T = 0.357) = 0.1032 \pm 0.0012$ from χ_{SG} and $h_{\text{AT}}(T = 0.357) = 0.1034 \pm 0.0013$ from ξ_{SG} (see Table II for details).

where

$$\chi_{ij}^{\mu\nu} = \langle S_i^\mu S_j^\nu \rangle - \langle S_i^\mu \rangle \langle S_j^\nu \rangle. \quad (9)$$

From it the spin glass correlation length is then determined using the relation

$$\xi_{\text{SG}} = \frac{1}{2 \sin(k_{\min}/2)} \left(\frac{\chi_{\text{SG}}(0)}{\chi_{\text{SG}}(k_{\min})} - 1 \right)^{1/(2\sigma-1)}, \quad (10)$$

and $k_{\min} = 2\pi/N$. The spin glass susceptibility itself $\chi_{\text{SG}} = \chi_{\text{SG}}(0)$. The simulations and checks for equilibration were done following the procedures given in Ref. [9, 28].

At the AT transition, both χ_{SG} and ξ_{SG} diverge to infinity. For $\sigma < 2/3$ the finite size scaling forms when approaching the AT line along a vertical trajectory (i.e. by varying h_r) takes the form for a finite value of N [23]

$$\frac{\chi_{\text{SG}}}{N^{1/3}} = \mathcal{C} \left[N^{1/3} (h_r - h_{\text{AT}}(T)) \right] + N^{-\omega} \mathcal{G} \left[N^{1/3} (h_r - h_{\text{AT}}(T)) \right]. \quad (11)$$

The second term is a correction to scaling term. The exponent ω is given by [9, 29]

$$\omega = 1/3 - (2\sigma - 1). \quad (12)$$

Notice that as $\sigma \rightarrow 2/3$, $\omega \rightarrow 0$. This is why it is so challenging to show that the AT line disappears as $d \rightarrow 6$. The finite size scaling form for ξ_{SG} is [23]

$$\frac{\xi_{\text{SG}}}{N^{d_{\text{eff}}/6}} = \mathcal{X} \left[N^{1/3} (h_r - h_{\text{AT}}(T)) \right] + N^{-\omega} \mathcal{H} \left[N^{1/3} (h_r - h_{\text{AT}}(T)) \right]. \quad (13)$$

In the absence of the correction to scaling term the plots of $\chi_{\text{SG}}/N^{1/3}$ or $\xi_{\text{SG}}/N^{d_{\text{eff}}/6}$ for different system sizes would intersect at $h_r = h_{\text{AT}}(T)$. The intersection formula for the successive crossing points $h^*(N, 2N)$ should be linear in $1/N^\lambda$ when $N \rightarrow \infty$ and be of the form

$$h^*(N, 2N) = h_{\text{AT}}(T) + \frac{A}{N^\lambda}, \quad (14)$$

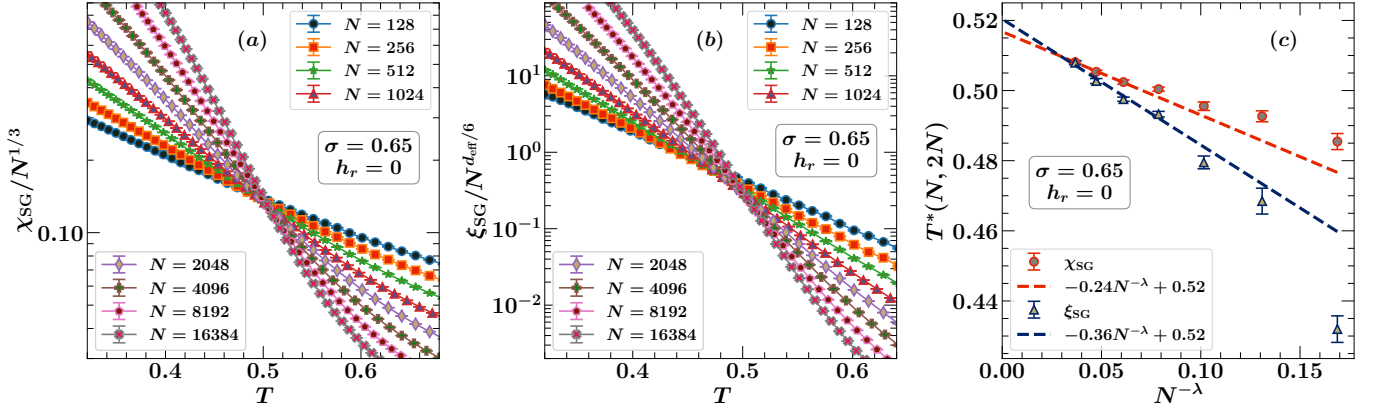


FIG. 8. Finite size scaling analyses of (a) χ_{SG} data, and (b) ξ_{SG} data, for $\sigma = 0.650$ obtained by varying the temperature in the absence of a magnetic field. The data for the intersection temperatures $T^*(N, 2N)$ are plotted as a function of $N^{-\lambda}$ (using $\lambda = 0.367$) in (c). The values of the zero-field transition temperature obtained from linear fitting are $T_c = 0.5168 \pm 0.0012$ from χ_{SG} and $T_c = 0.5204 \pm 0.0012$ from ξ_{SG} (see Table I for details).

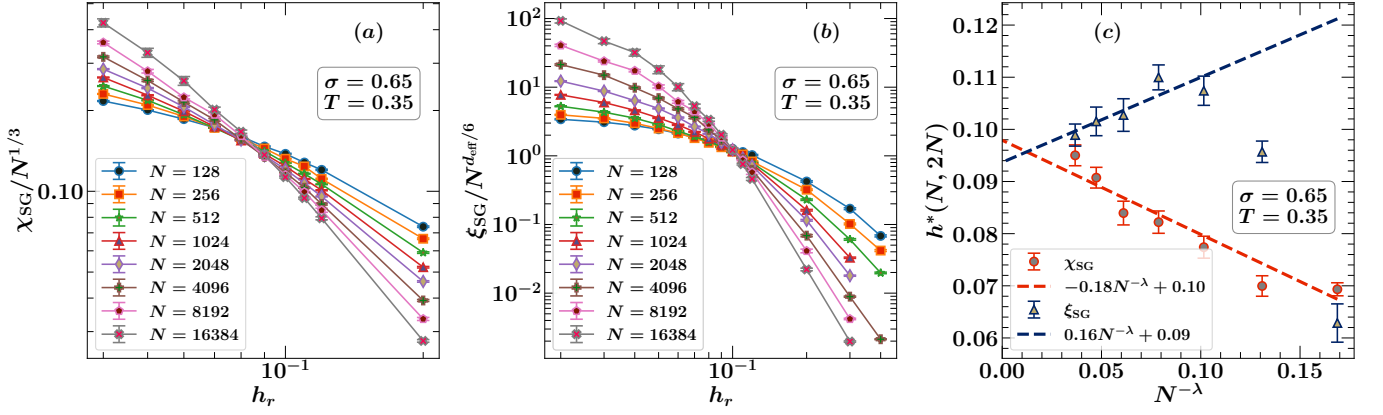


FIG. 9. Finite size scaling analyses of (a) χ_{SG} data, and (b) ξ_{SG} data, for $\sigma = 0.650$ obtained by fixing the temperature to $T = 0.350 (= 0.675 T_c)$ and varying the field. (c) shows the data for the intersection fields $h^*(N, 2N)$ between pairs of adjacent system sizes, plotted as a function of $N^{-\lambda}$. Using $\lambda = 0.367$ we fitted the $h^*(N, 2N)$ data linearly with Eq. (14) and the values of the transition field so obtained are $h_{AT}(T = 0.350) = 0.0979 \pm 0.0016$ from χ_{SG} and $h_{AT}(T = 0.350) = 0.0937 \pm 0.0033$ from ξ_{SG} (see Table II for details).

where

$$\lambda = 1/3 + \omega. \quad (15)$$

We have not only studied χ_{SG} and ξ_{SG} as a function of h_r at fixed T we have also studied them as a function of T for fixed $h_r = 0$. We did the latter to determine the zero-field transition temperature T_c . The relevant finite size scaling forms for this situation are

$$\frac{\chi_{SG}}{N^{1/3}} = \tilde{\mathcal{C}} \left[N^{1/3}(T - T_c) \right] + N^{-\omega} \tilde{\mathcal{G}} \left[N^{1/3}(T - T_c) \right], \quad (16)$$

and

$$\frac{\xi_{SG}}{N^{d_{eff}/6}} = \tilde{\mathcal{X}} \left[N^{1/3}(T - T_c) \right] + N^{-\omega} \tilde{\mathcal{H}} \left[N^{1/3}(T - T_c) \right]. \quad (17)$$

The tilde sign is to indicate that the finite size scaling functions such as \mathcal{C} in a field and $\tilde{\mathcal{C}}$ in the absence of a field may differ.

The intersection points as in, say, Fig.4 (c) would be expected to be of the form

$$T^*(N, 2N) = T_c + \frac{\tilde{A}}{N^\lambda}. \quad (18)$$

Note that the values of the exponents ω and λ are the same for the zero field transition and for the AT line (assuming that they are both governed by a Gaussian fixed point).

In the section IV we give the results of our studies of both χ_{SG} and ξ_{SG} for values of σ at 0.600, 0.630, 0.640, 0.650 and 0.655. We also describe how the zero-field transition temperature T_c was determined for each of these values of σ .

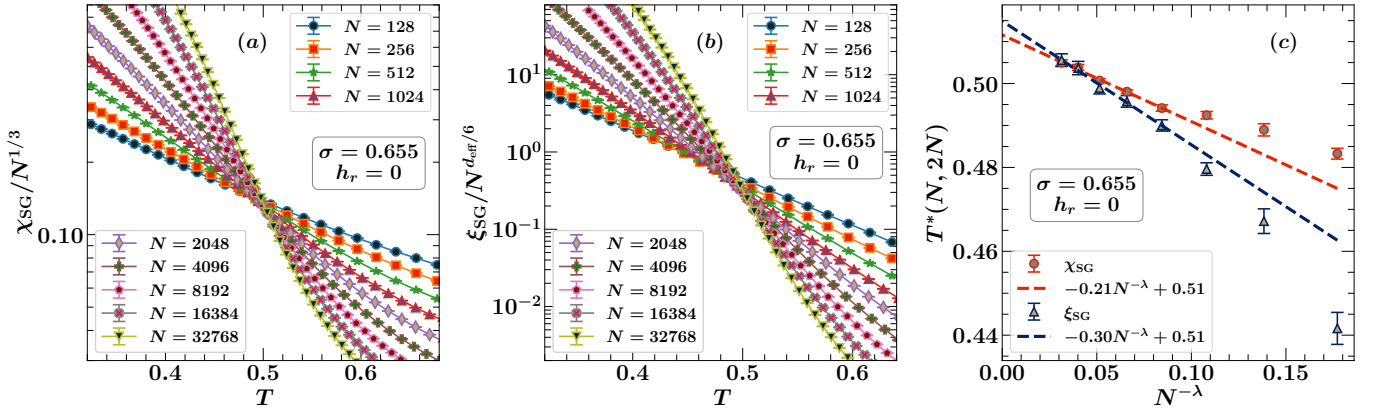


FIG. 10. Finite size scaling analyses of χ_{SG} data, and ξ_{SG} data, for $\sigma = 0.655$ obtained by varying the temperature in the absence of a magnetic field. (c) shows the data for the intersection temperatures $T^*(N, 2N)$ fitted against $N^{-\lambda}$. The value of the exponent λ is fixed to be 0.357. The fits give $T_c = 0.5116 \pm 0.0009$ from χ_{SG} and $T_c = 0.5149 \pm 0.0020$ from ξ_{SG} (see Table I for details).

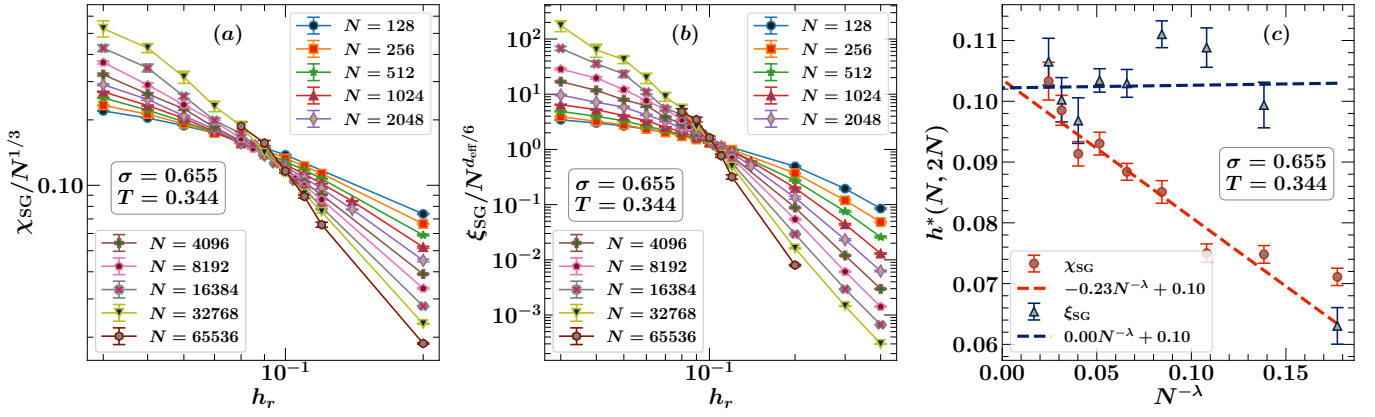


FIG. 11. Finite size scaling analyses of (a) χ_{SG} data, and (b) ξ_{SG} data, for $\sigma = 0.655$ obtained by fixing the temperature to $T = 0.344 (= 0.675 T_c)$ and varying the field. In (c) the data for the intersection fields $h^*(N, 2N)$ is plotted as a function of $N^{-\lambda}$ with $\lambda = 0.357$. We fitted the $h^*(N, 2N)$ data with a straight line and the values of the transition field obtained as a result of the extrapolation of the lines are $h_{\text{AT}}(T = 0.344) = 0.1036 \pm 0.0015$ from χ_{SG} and $h_{\text{AT}}(T = 0.344) = 0.1022 \pm 0.0061$ from ξ_{SG} (see Table II for details).

IV. FINITE SIZE SCALING ANALYSES

Here we give further details of the results of our simulations for σ values 0.600, 0.630, 0.640, 0.650 and 0.655. Figs. 4, 6, 8, and 10 show the finite size scaling analyses of data for these different values of σ obtained by varying the temperature in the absence of a magnetic field. In all these figures, Figs. (a) show the plot of $\chi_{\text{SG}}/N^{1/3}$ as a function of the temperature T for different system sizes. The corresponding data for $\xi_{\text{SG}}/N^{d_{\text{eff}}/6}$ are shown in Figs. (b), with $d_{\text{eff}} = 2/(2\sigma - 1)$ in the mean-field regime. In all these sets of plots we can clearly notice that the curves for different system sizes intersect around the transition temperature, which is in accordance with Eqs. (16) and (17). For each pair of adjacent system sizes, we find the intersection temperature $T^*(N, 2N)$ from both χ_{SG} and ξ_{SG} data which is the x -coordinate corresponding to the point of intersection between

these curves. The data for the intersection temperatures obtained from all the pairs of adjacent system sizes are plotted as a function of $N^{-\lambda}$ in Figs. (c). The value of the exponent λ is known in the mean-field regime and is given by Eq. (15) [24, 25]. Using this value of λ we fit the $T^*(N, 2N)$ data linearly with Eq. (18). In the thermodynamic limit $N^{-\lambda} \rightarrow 0$ as $N \rightarrow \infty$. Hence, the y -intercept corresponding to the straight line fit gives us the value of the zero-field transition temperature T_c . We get two values for T_c , one from χ_{SG} and the other from ξ_{SG} data, which are in agreement with each other within the errorbars. The values of T_c obtained for different values of σ are shown in Table I, and the parameters of the simulations are shown in Table AI.

The AT line can be approached not only by reducing the temperature T but also by reducing the field at fixed T . This was the procedure used in Ref. [23]. These are the vertical trajectories in Fig. 1 along which we can

TABLE I. Results of the simulations done by varying the temperature T in the absence of magnetic field h_r . The $\chi_{\text{SG}}/N^{1/3}$ (or $\xi_{\text{SG}}/N^{d_{\text{eff}}/6}$, with $d_{\text{eff}} = 2/(2\sigma - 1)$), when plotted as a function of temperature T , the data for different system sizes N intersect around the transition temperature $T_c(\chi_{\text{SG}})$ (or $T_c(\xi_{\text{SG}})$). The intersection temperatures $T^*(N, 2N)$ between the curves for two adjacent system sizes are then plotted as a function of $N^{-\lambda}$, with $\lambda = 5/3 - 2\sigma$ in the mean field regime [24, 25]. We then fit this data for the N_{pairs} largest pairs of system sizes with Eq. (18) to find the transition temperature $T_c(\chi_{\text{SG}})$ (or $T_c(\xi_{\text{SG}})$).

σ	h_r	λ	$N_{\text{pairs}}(\chi_{\text{SG}})$	$T_c(\chi_{\text{SG}})$	$N_{\text{pairs}}(\xi_{\text{SG}})$	$T_c(\xi_{\text{SG}})$
0.600	0	0.467	5	0.5609 ± 0.0012	7	0.5617 ± 0.0021
0.630	0	0.407	3	0.5405 ± 0.0024	3	0.5405 ± 0.0045
0.640	0	0.387	4	0.5244 ± 0.0020	4	0.5326 ± 0.0038
0.650	0	0.367	3	0.5168 ± 0.0012	4	0.5204 ± 0.0012
0.655	0	0.357	5	0.5116 ± 0.0009	5	0.5149 ± 0.0020

TABLE II. Results of the simulations done by varying the magnetic field h_r at a fixed temperature $T = 0.675 T_c$, where T_c is the zero-field spin glass transition temperature. Similar to the fixed h_r case described in Table I, we plot the finite-size-scaled χ_{SG} (or ξ_{SG}) data as a function of the field h_r and find the intersection fields $h^*(N, 2N)$. We then fit this data with Eq. (14) to find the AT transition field h_{AT} corresponding to the temperature T .

σ	T_c	T	λ	$N_{\text{pairs}}(\chi_{\text{SG}})$	$h_{\text{AT}}(\chi_{\text{SG}})$	$N_{\text{pairs}}(\xi_{\text{SG}})$	$h_{\text{AT}}(\xi_{\text{SG}})$
0.600	0.563	0.380	0.467	4	0.1287 ± 0.0033	7	0.1327 ± 0.0015
0.630	0.540	0.364	0.407	7	0.1094 ± 0.0012	6	0.1081 ± 0.0015
0.640	0.530	0.357	0.387	6	0.1032 ± 0.0012	6	0.1034 ± 0.0013
0.650	0.519	0.350	0.367	7	0.0979 ± 0.0016	5	0.0937 ± 0.0033
0.655	0.510	0.344	0.357	8	0.1036 ± 0.0015	4	0.1022 ± 0.0061

cross the AT line. Throughout this paper, we chose the value of temperature T such that $T/T_c = 0.675$. We show our finite size scaling analyses plots corresponding to this procedure in Figs. 3, 5, 7, 9, and 11. Similar to the zero-magnetic field case, we present our χ_{SG} and ξ_{SG} data in Figs. (a) and (b) as a function of magnetic field h_r . According to Eq. (11), the data for $\chi_{\text{SG}}/N^{1/3}$ when plotted for different system sizes should intersect at the AT transition field $h_{\text{AT}}(T)$. Similarly, according to Eq. (13), the data of $\xi_{\text{SG}}/N^{d_{\text{eff}}/6}$ with $d_{\text{eff}} = 2/(2\sigma - 1)$ should intersect at the same transition field. Figs. (c) show the data for the intersection fields $h^*(N, 2N)$ obtained by considering the curves for adjacent system sizes. We fit the $h^*(N, 2N)$ data with Eq. (14) through a straight line using the same value of λ as in the previous scenario, which is given by Eq. (15). The point at which this straight line cuts the y -axis gives us the value of the transition field h_{AT} corresponding to the temperature T . If the values of h_{AT} obtained from both χ_{SG} and ξ_{SG} agree with each other within the permissible error limits for the data, we say that there is a phase transition in the system for that value of σ corresponding to the temperature T . The values of h_{AT} obtained for different σ are shown in Table II, and the parameters of the simulation are shown in Table AII. In the following sections we present the values of T_c and $h_{\text{AT}}(T = 0.675 T_c)$ for different values of σ .

A. $\sigma = 0.600$

At $\sigma = 0.600$, for which $d_{\text{eff}} = 10$ the results should be quite close to those of the SK model (but see Fig. 1): it is in the same mean-field regime and the exponent $\zeta = 3$. The zero-field transitions for this case has been studied by one of the authors of this paper in Ref. [24] for Heisenberg spins. The value of the zero-field spin glass transition temperature found from these simulations is $T_c = 0.563$. The phase transitions in the presence of an external magnetic field has also been studied in Ref. [30] for $h_r = 0.1$. It has been reported that the system undergoes a phase transition at $T_{\text{AT}}(h_r = 0.1) = 0.406$.

For $\sigma = 0.600$ we fixed the temperature at $T = 0.380 (= 0.675 T_c)$. We have constructed the crossing plots for χ_{SG} and ξ_{SG} as a function of h_r in Figs. 3(a) and 3(b), respectively. Analysis of the crossing points $h^*(N, 2N)$ in Fig. 3(c) shows that the behavior is again consistent with the existence of an AT line at least at $\sigma = 0.600$. The value of the exponent λ is known in the mean-field regime and is given by $\lambda = 5/3 - 2\sigma = 0.467$. The $h^*(N, 2N)$ data for the largest 4 pairs of system sizes are fitted against $N^{-\lambda}$ to give $h_{\text{AT}}(T = 0.380) = 0.1287 \pm 0.0033$ from χ_{SG} and $h_{\text{AT}}(T = 0.380) = 0.1327 \pm 0.0015$ from ξ_{SG} (omitting the smallest system size). The values of h_{AT} obtained from χ_{SG} data and ξ_{SG} data are in agreement with each other within the error bars.

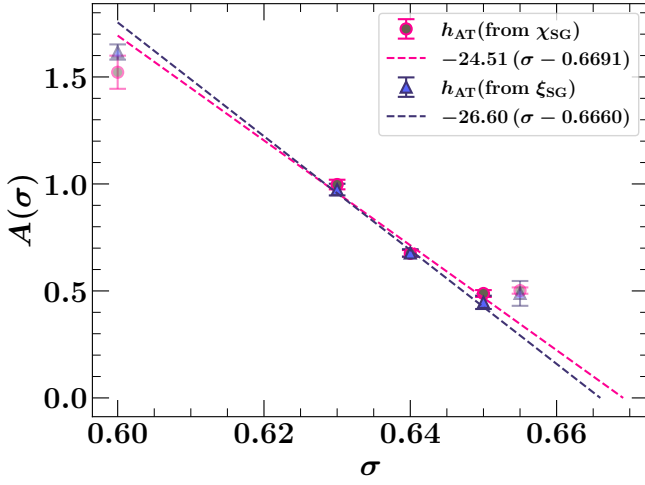


FIG. 12. Plot of $A(\sigma)$ versus σ . The quantity $A(\sigma)$ is computed using Eq. (1) with the exponent ζ given by Eq. (19) in the mean-field regime. In our simulations we fixed the temperature $T = 0.675T_c$ and determined the value of the transition field h_{AT} from the χ_{SG} and ξ_{SG} data sets, (for example see Fig. 5). So, for each σ , we get two values of $A(\sigma)$ corresponding to the two different values of h_{AT} . The $A(\sigma)$ data corresponding to $\sigma = 0.630, 0.640$, and 0.650 are fitted with a straight line. The red and blue lines intersect the σ -axis at $\sigma = 0.669 \pm 0.072$ and $\sigma = 0.666 \pm 0.101$ respectively. In making these linear fits the data point at $\sigma = 0.60$ has been ignored, as it will lie outside the linear region which only applies for σ values close to $2/3$. The data point at $\sigma = 0.655$ was judged to be too badly affected by finite size effects to be included in the linear fit. The error bars are the statistical error bars, but finite size effects produce an unknown systematic error in all the data points.

B. $\sigma = 0.630$

For $\sigma = 0.630$ $d_{\text{eff}} \approx 7.692$. Our results for $h_r = 0$ are given in Fig. 4. According to Eq. (16), the data for $\chi_{SG}/N^{1/3}$ when plotted for different system sizes should intersect at the transition temperature T_c . Similarly, according to Eq. (17), the data of $\xi_{SG}/N^{d_{\text{eff}}/6}$ with $d_{\text{eff}} = 2/(2\sigma - 1)$ should intersect at the same transition temperature. Figs. 4(a) and 4(b) show the data for different system sizes. We find the temperature $T^*(N, 2N)$ at which the curves corresponding to the system sizes N and $2N$ intersect. We then fit this data with Eq. (18) to find the transition temperature. The exponent $\lambda \equiv 5/3 - 2\sigma$ is known to equal 0.407 in this case. The result is displayed in Fig. 4(c), where the $T^*(N, 2N)$ data obtained from intersections of χ_{SG} are fitted against $N^{-\lambda}$ with a straight line for the largest 3 pairs of system sizes to give $T_c = 0.5405 \pm 0.0024$. The corresponding intersections of the ξ_{SG} data (considering the 3 largest system sizes) give $T_c = 0.5405 \pm 0.0045$. The values of T_c obtained from χ_{SG} data and ξ_{SG} data are in agreement with each other.

We have also studied χ_{SG} and ξ_{SG} at fixed T , but varying h_r and the finite size scaling plots for these are

given in Figs. 5(a) and 5(b). There appears to be good intersections in the curves, supporting therefore the possible existence of an AT transition at the temperature studied $T = 0.364$. A plot of $h^*(N, 2N)$ versus $1/N^\lambda$ is in Fig. 5(c), using the same value of $\lambda = 0.407$. Considering the data for the 7 largest pairs of system sizes, we did a linear fitting over the $h^*(N, 2N)$ data obtained from χ_{SG} intersections, which gives $h_{AT}(T = 0.364) = 0.1094 \pm 0.0012$. Similarly, the ξ_{SG} intersections, considering the 6 pairs of largest system sizes, give $h_{AT}(T = 0.364) = 0.1081 \pm 0.0015$.

C. $\sigma = 0.640$

For $\sigma = 0.640$, $d_{\text{eff}} \approx 7.143$. Our results for $h_r = 0$ are given in Fig. 6. Figs. 6(a) and 6(b) show the χ_{SG} and ξ_{SG} data respectively for different system sizes, and the corresponding intersection temperatures data are displayed in Fig. 6(c). The value of the exponent λ for this case is 0.387. The linear fit over the $T^*(N, 2N)$ data obtained from intersections of χ_{SG} , considering the 4 pairs of largest system sizes, give $T_c = 0.5244 \pm 0.0020$. The corresponding intersections of the ξ_{SG} data (omitting the 3 smallest system sizes) give $T_c = 0.5326 \pm 0.0038$. The values of T_c obtained from χ_{SG} data and ξ_{SG} data are in agreement with each other (see Table I).

As for the alternate protocol where we fix the temperature and vary the field, the finite size scaling plots are given in Figs. 7(a) and 7(b). The temperature is fixed at $T = 0.357 (= 0.675T_c)$. A plot of $h^*(N, 2N)$ versus $1/N^\lambda$ is in Fig. 7(c), using the same value of $\lambda = 0.387$. Omitting the smallest system size, we did a linear fitting over the $h^*(N, 2N)$ data obtained from χ_{SG} intersections, which gives $h_{AT}(T = 0.357) = 0.1032 \pm 0.0012$. Similarly, the ξ_{SG} intersections, considering the 6 largest system sizes, give $h_{AT}(T = 0.357) = 0.1034 \pm 0.0013$.

D. $\sigma = 0.650$

For $\sigma = 0.650$ $d_{\text{eff}} \approx 6.667$. Our results for $h_r = 0$ are given in Fig. 8. Figs. 8(a) and 8(b) show the χ_{SG} and ξ_{SG} data for different system sizes. We find the temperature $T^*(N, 2N)$ and fit this data with Eq. (18) to find the transition temperature. The exponent $\lambda \equiv 5/3 - 2\sigma$ is known to equal 0.367 in this case [24, 25]. The result is displayed in Fig. 8(c), where the $T^*(N, 2N)$ data obtained from intersections of χ_{SG} are fitted against $N^{-\lambda}$ with a straight line for the largest 3 pairs of system sizes to give $T_c = 0.5168 \pm 0.0012$. The corresponding intersections of the ξ_{SG} data (omitting the 3 smallest system sizes) give $T_c = 0.5204 \pm 0.0012$. The values of T_c obtained from χ_{SG} data and ξ_{SG} data are in agreement with each other (see Table I).

We have also studied ξ_{SG} and χ_{SG} at fixed temperature $T = 0.350 (= 0.675T_c)$, but varying h_r and the finite size scaling plots for these are given in Figs. 11(a) and

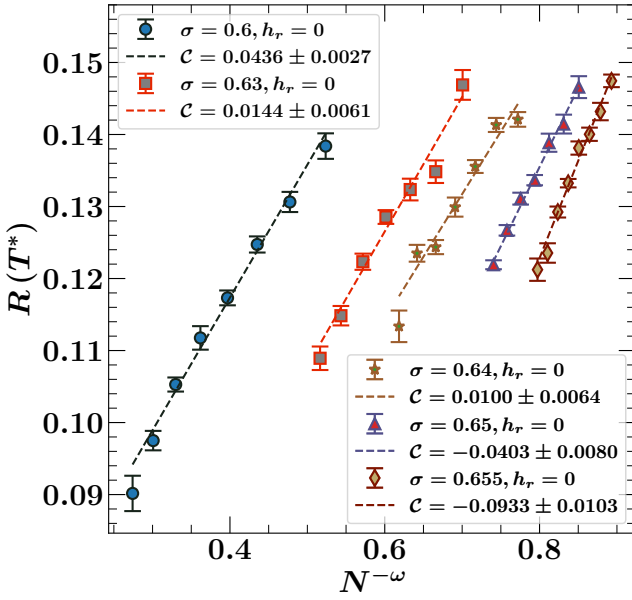


FIG. 13. The values of $R(T^*) = \chi_{\text{SG}}(T^*(N, 2N), N)/N^{1/3}$ for the range of σ values studied in this paper, in zero field. The correction to scaling exponent $\omega = 1/3 - (2\sigma - 1)$. \mathcal{C} is the value of R obtained using the dotted line extrapolation. As $\sigma \rightarrow 2/3$ the values of N needed to estimate the value of R accurately has to increase rapidly.

11(b). A plot of $h^*(N, 2N)$ versus $1/N^\lambda$ is in Fig. 9(c), using the same value of $\lambda = 0.367$. Omitting the smallest system size, the linear fit from χ_{SG} intersections give $h_{\text{AT}}(T = 0.350) = 0.0979 \pm 0.0016$. Similarly, the ξ_{SG} intersections, considering the 5 largest system sizes, give $h_{\text{AT}}(T = 0.350) = 0.0937 \pm 0.0033$.

E. $\sigma = 0.655$

For $\sigma = 0.655$ $d_{\text{eff}} \approx 6.452$. Our results for $h_r = 0$ are given in Fig. 10. The $\chi_{\text{SG}}/N^{1/3}$ and $\xi_{\text{SG}}/N^{d_{\text{eff}}/6}$ data are plotted as a function of temperature T in figs. 10(a) and 10(b) respectively, for different system sizes. We find the temperature $T^*(N, 2N)$ at which the curves corresponding to the system sizes N and $2N$ intersect. We then fit this data with Eq. (18) to find the transition temperature. The exponent $\lambda \equiv 5/3 - 2\sigma$ is known to equal 0.357 in this case [24, 25]. The result is displayed in Fig. 10(c), where the $T^*(N, 2N)$ data obtained from intersections of χ_{SG} are fitted against $N^{-\lambda}$ with a straight line for the largest 5 pairs of system sizes to give $T_c = 0.5116 \pm 0.0009$. The corresponding intersections of the ξ_{SG} data (omitting the 3 smallest system sizes) give $T_c = 0.5149 \pm 0.0020$. The values of T_c obtained from χ_{SG} data and ξ_{SG} data are in agreement with each other.

We have also studied ξ_{SG} and χ_{SG} at fixed $T = 0.344 (= 0.675T_c)$, but varying h_r and the finite size scaling plots for these are given in Figs. 9(a) and 9(b). A plot of

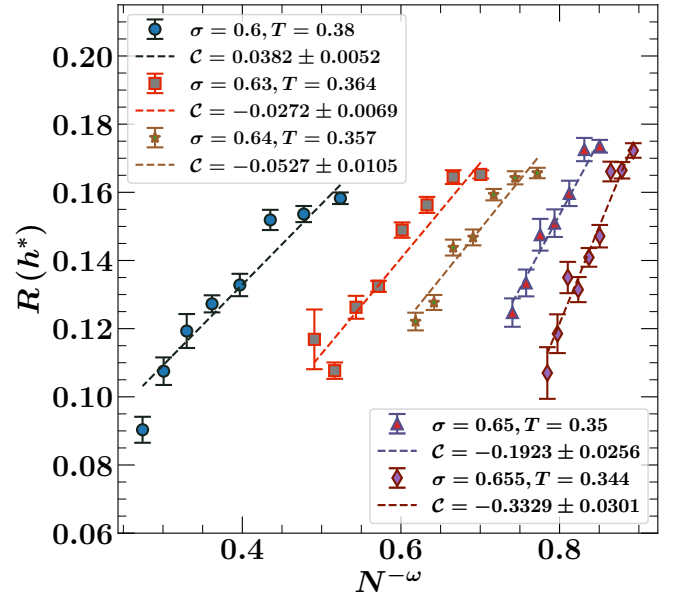


FIG. 14. The values of $R(h^*) = \chi_{\text{SG}}(h^*(N, 2N), N)/N^{1/3}$ for the range of σ values studied in this paper at the temperatures previously used. The correction to scaling exponent $\omega = 1/3 - (2\sigma - 1)$. \mathcal{C} is the value of R obtained using the dotted line extrapolation. Only the data at $\sigma = 0.60$ extrapolates to a positive value.

$h^*(N, 2N)$ versus $1/N^\lambda$ is in Fig. 9(c), using the same value of $\lambda = 0.357$. Omitting the smallest system size, we did a linear fitting over the $h^*(N, 2N)$ data obtained from χ_{SG} intersections, which gives $h_{\text{AT}}(T = 0.344) = 0.1036 \pm 0.0015$. Similarly, the ξ_{SG} intersections, considering the 4 largest system sizes, give $h_{\text{AT}}(T = 0.344) = 0.1022 \pm 0.0061$.

V. DISAPPEARANCE OF THE AT LINE AS $\sigma \rightarrow 2/3$

In this section we present our analysis of $A(\sigma)$ for different values of $\sigma < 2/3$, and with the help of this data, we show that the AT line approaches the horizontal axis as we go below six dimensions, or equivalently for $\sigma > 2/3$. As shown in Table II, for each σ , we get two estimates of the value of AT transition field h_{AT} for a fixed temperature T ; one from χ_{SG} and one from ξ_{SG} . From it, one can extract (using Eq. (1)) $A(\sigma)$ at the values of σ which we have studied. We take the exponent to be:

$$\zeta = \begin{cases} 3, & \sigma < 5/8, \\ \frac{2(1-\sigma)}{2\sigma-1}, & 5/8 < \sigma < 2/3, \end{cases} \quad (19)$$

where we have set $d = d_{\text{eff}}$ in $\zeta = d/2 - 1$ for $\sigma > 5/8$ [6, 7]. We have plotted the results in Fig. 12. Clearly $A(\sigma)$ is decreasing with increasing σ , and in this linear plot it appears to go to zero when $\sigma \approx 0.67$. This is close

to the value $2/3$ which is what would be expected if the AT line disappears in exactly 6 dimensions.

When we studied $\sigma = 0.655$, we saw a deviation from the straight line which goes through $\sigma \approx 0.67$ in Fig. 12. We believe the basic reason for this deviation are finite size problems. Finite size effects give an apparent AT transition at values of σ where it is actually absent! The same finite size effects made h_{AT} finite at $d = 6$ in [22]. In our study of the XY model [23] we also studied the cases $\sigma = 0.70, 0.75$ and 0.85 . These correspond to dimensions $d < 6$ and in the region where the droplet scaling approach should work and where there will be no AT transition. However, there were still intersections of the lines of χ_{SG} and ξ_{SG} for different N values which at first sight suggests the presence of an AT transition and a non-vanishing value of h_{AT} . However, by studying the N dependence of these intersections one could see that they do not correspond to a phase transition but are consequences of finite size effects. We believe that is why an AT transition was reported in the recent study in which a system with $d = 6$ was simulated [22] and why the data point at $\sigma = 0.655$ should be discounted.

To appreciate the size of finite size corrections for the zero field case it is useful to study R where

$$R \equiv \frac{\chi_{\text{SG}}(T^*(N, 2N), N)}{N^{1/3}}. \quad (20)$$

R is the righthand side of Eq. (16). The first term has been calculated analytically [31] and is always positive and independent of σ when $\sigma < 2/3$. Because we only determine $\chi_{\text{SG}}(T, N)$ at a finite number of values of T , we use linear interpolation to calculate $\chi_{\text{SG}}(T^*(N, 2N), N)$ using the two points which lie on either side of $T^*(N, 2N)$. R should therefore approach the same positive constant as $1/N^\omega \rightarrow 0$ for all $\sigma < 2/3$. Fig. 13 shows that $1/N^\omega$ is still large at the system sizes which have been achieved in this study. Its value for $N = 32768$ at $\sigma = 0.655$ is 0.785 . The extrapolated value of R for $N \rightarrow \infty$ is not even positive for the two values of σ closest to $2/3$, i.e. 0.650 and 0.655 ! The fitting of $T^*(N, 2N)$ to a linear form in $1/N^\lambda$ to obtain T_c in plots like that of Fig. 4 (c) will only be valid when the second term in Eq. (16) can be approximated as *constant* $N^{-\omega}$ and the data for 0.650 and 0.655 shows that cannot be the case at least for these two values of σ . This will make for a systematic error in the determination of T_c .

The magnitude of the scaling corrections in a field is very similar to the zero field case and the absence of

good straight line fits in Figs. 5(c), 7(c), 9(c), and 11(c) is therefore to be expected. The system sizes studied are just not sufficiently large to see the simple finite size scaling forms cleanly emerging.

VI. SUMMARY AND CONCLUSIONS

Due to the challenges associated with performing simulations above six dimensions, we have opted to perform simulations using a one-dimensional proxy model instead. For the one dimensional Heisenberg spin glasses with power-law diluted interactions, we studied five values of $\sigma < 2/3$: $0.600, 0.630, 0.640, 0.650$, and 0.655 .

To find the values of the zero-field spin glass transition temperature T_c , we performed simulations by varying the temperature T in the absence of the magnetic field. We then fixed the temperature to $T = 0.675T_c$ and generated the data by varying the magnetic field for different values of σ . The largest system sizes studied are $N = 32768$ for $\sigma = 0.600$ and 0.630 , $N = 16384$ for $\sigma = 0.640$ and 0.650 , and $N = 65536$ for $\sigma = 0.655$. Using the standard finite size scaling analysis we found the values of the AT transition field h_{AT} , which gave us the values of $A(\sigma)$. When $A(\sigma)$ was studied as a function of σ , it is becoming zero for σ close to $2/3$. This is equivalent to saying that $A(d)$ is vanishing as we approach $d = 6$ from above six dimensions. The numerical studies reported in this paper imply therefore that the AT line is approaching the temperature axis as $d \rightarrow 6$, and hence that there will not be an AT transition below six dimensions.

Numerical studies like this can only provide evidence for what the truth might be: they do not as yet prove it beyond reasonable doubt. The controversy will probably only be ended by a rigorous determination of the lower critical dimension of the AT transition.

ACKNOWLEDGMENTS

We are grateful to the High Performance Computing (HPC) facility at IISER Bhopal, where large-scale calculations in this project were run. B.V is grateful to the Council of Scientific and Industrial Research (CSIR), India, for his PhD fellowship. A.S acknowledges financial support from SERB via the grant (File Number: CRG/2019/003447), and from DST via the DST-INSPIRE Faculty Award [DST/INSPIRE/04/2014/002461].

-
- [1] G. Parisi, "Toward a mean field theory for spin glasses," *Physics Letters A* **73**, 203–205 (1979).
 - [2] Marc Mézard, Giorgio Parisi, and Miguel Angel Virasoro, *Spin glass theory and beyond: An Introduction to the Replica Method and Its Applications*, Vol. 9 (World

Scientific Publishing Company, 1986).

- [3] A J Bray and S A Roberts, "Renormalisation-group approach to the spin glass transition in finite magnetic fields," *Journal of Physics C: Solid State Physics* **13**, 5405 (1980).

- [4] J R L de Almeida and D J Thouless, “Stability of the Sherrington-Kirkpatrick solution of a spin glass model,” *Journal of Physics A: Mathematical and General* **11**, 983–990 (1978).
- [5] David Sherrington and Scott Kirkpatrick, “Solvable Model of a Spin-Glass,” *Phys. Rev. Lett.* **35**, 1792–1796 (1975).
- [6] J E Green, M A Moore, and A J Bray, “Upper critical dimension for the de Almeida-Thouless instability in spin glasses,” *Journal of Physics C: Solid State Physics* **16**, L815 (1983).
- [7] Daniel S. Fisher and H. Sompolinsky, “Scaling in Spin-Glasses,” *Phys. Rev. Lett.* **54**, 1063–1066 (1985).
- [8] A. B. Harris, T. C. Lubensky, and Jing-Huei Chen, “Critical Properties of Spin-Glasses,” *Phys. Rev. Lett.* **36**, 415–418 (1976).
- [9] Auditya Sharma and A. P. Young, “de Almeida–Thouless line in vector spin glasses,” *Phys. Rev. E* **81**, 061115 (2010).
- [10] M A Moore and A J Bray, “The nature of the spin-glass phase and finite size effects,” *Journal of Physics C: Solid State Physics* **18**, L699 (1985).
- [11] Joonhyun Yeo and M. A. Moore, “Critical point scaling of Ising spin glasses in a magnetic field,” *Phys. Rev. B* **91**, 104432 (2015).
- [12] T. Aspelmeier, M. A. Moore, and A. P. Young, “Interface Energies in Ising Spin Glasses,” *Phys. Rev. Lett.* **90**, 127202 (2003).
- [13] T. Aspelmeier, Wenlong Wang, M. A. Moore, and Helmut G. Katzgraber, “Interface free-energy exponent in the one-dimensional Ising spin glass with long-range interactions in both the droplet and broken replica symmetry regions,” *Phys. Rev. E* **94**, 022116 (2016).
- [14] A. C. Carter, A. J. Bray, and M. A. Moore, “Aspect-Ratio Scaling and the Stiffness Exponent θ for Ising Spin Glasses,” *Phys. Rev. Lett.* **88**, 077201 (2002).
- [15] Alexander K. Hartmann, Alan J. Bray, A. C. Carter, M. A. Moore, and A. P. Young, “Stiffness exponent of two-dimensional Ising spin glasses for nonperiodic boundary conditions using aspect-ratio scaling,” *Phys. Rev. B* **66**, 224401 (2002).
- [16] Wenlong Wang, M. A. Moore, and Helmut G. Katzgraber, “Fractal dimension of interfaces in Edwards-Anderson spin glasses for up to six space dimensions,” *Phys. Rev. E* **97**, 032104 (2018).
- [17] Stefan Boettcher, “Stiffness of the Edwards-Anderson Model in all Dimensions,” *Phys. Rev. Lett.* **95**, 197205 (2005).
- [18] M. A. Moore, “ $1/m$ expansion in spin glasses and the de Almeida-Thouless line,” *Phys. Rev. E* **86**, 031114 (2012).
- [19] J. Mattsson, T. Jonsson, P. Nordblad, H. Aruga Katori, and A. Ito, “No Phase Transition in a Magnetic Field in the Ising Spin Glass $\text{Fe}_{0.5}\text{Mn}_{0.5}\text{TiO}_3$,” *Phys. Rev. Lett.* **74**, 4305–4308 (1995).
- [20] V. S. Zotev, G. G. Kenning, and R. Orbach, “From linear to nonlinear response in spin glasses: Importance of mean-field-theory predictions,” *Phys. Rev. B* **66**, 014412 (2002).
- [21] V. Martin-Mayor, J. J. Ruiz-Lorenzo, B. Seoane, and A. P. Young, “Numerical Simulations and Replica Symmetry Breaking,” (2022), [arXiv:2205.14089 \[cond-mat.dis-nn\]](#).
- [22] Miguel Aguilar-Janita, Victor Martin-Mayor, Javier Moreno-Gordo, and Juan Jesus Ruiz-Lorenzo, “Second order phase transition in the six-dimensional Ising spin glass on a field,” (2023), [arXiv:2306.00569 \[cond-mat.dis-nn\]](#).
- [23] Bharadwaj Vedula, M. A. Moore, and Auditya Sharma, “Study of the de Almeida–Thouless line in the one-dimensional diluted power-law XY spin glass,” *Phys. Rev. E* **108**, 014116 (2023).
- [24] Auditya Sharma and A. P. Young, “Phase transitions in the one-dimensional long-range diluted Heisenberg spin glass,” *Phys. Rev. B* **83**, 214405 (2011).
- [25] Derek Larson, Helmut G. Katzgraber, M. A. Moore, and A. P. Young, “Numerical studies of a one-dimensional three-spin spin-glass model with long-range interactions,” *Phys. Rev. B* **81**, 064415 (2010).
- [26] Helmut G. Katzgraber and A. P. Young, “Monte Carlo studies of the one-dimensional Ising spin glass with power-law interactions,” *Phys. Rev. B* **67**, 134410 (2003).
- [27] L. Leuzzi, G. Parisi, F. Ricci-Tersenghi, and J. J. Ruiz-Lorenzo, “Dilute One-Dimensional Spin Glasses with Power Law Decaying Interactions,” *Phys. Rev. Lett.* **101**, 107203 (2008).
- [28] L. W. Lee and A. P. Young, “Large-scale Monte Carlo simulations of the isotropic three-dimensional Heisenberg spin glass,” *Phys. Rev. B* **76**, 024405 (2007).
- [29] Derek Larson, Helmut G. Katzgraber, M. A. Moore, and A. P. Young, “Numerical studies of a one-dimensional three-spin spin-glass model with long-range interactions,” *Phys. Rev. B* **81**, 064415 (2010).
- [30] Auditya Sharma and A. P. Young, “de Almeida–Thouless line studied using one-dimensional power-law diluted Heisenberg spin glasses,” *Phys. Rev. B* **84**, 014428 (2011).
- [31] T. Aspelmeier, Helmut G. Katzgraber, Derek Larson, M. A. Moore, Matthew Wittmann, and Joonhyun Yeo, “Finite-size critical scaling in Ising spin glasses in the mean-field regime,” *Phys. Rev. E* **93**, 032123 (2016).

Appendix A: Parameters of the simulations

TABLE AI. Parameters of the simulations. N_{samp} is the number of disorder samples, N_{sweep} is the number of over-relaxation Monte Carlo sweeps for a single disorder sample. The system is equilibrated over the first half of the sweeps, and measurements are done over the last half of the sweeps with a measurement performed every four over-relaxation sweeps. T_{min} and T_{max} are the lowest and highest temperatures simulated, and N_T is the number of temperatures used for parallel tempering. t_{tot} is the total CPU time consumed in hours to generate data for a particular system size.

σ	h_r	N	N_{samp}	N_{sweep}	T_{min}	T_{max}	N_T	t_{tot} (hrs)
0.6	0	128	12000	256	0.2	0.7	40	1.2
0.6	0	256	12000	512	0.2	0.7	40	4.89
0.6	0	512	12000	1024	0.2	0.7	40	21.57
0.6	0	1024	12000	2048	0.2	0.7	40	48.58
0.6	0	2048	9600	4096	0.2	0.7	40	235.21
0.6	0	4096	7200	8192	0.3	0.7	40	1109.96
0.6	0	8192	3120	16384	0.3	0.7	50	2611.03
0.6	0	16384	1200	32768	0.35	0.7	55	6453.1
0.6	0	32768	408	65536	0.35	0.7	60	7663.65
0.63	0	128	8000	512	0.2	0.7	40	1.24
0.63	0	256	8000	1024	0.2	0.7	40	5.81
0.63	0	512	8000	2048	0.2	0.7	40	29.16
0.63	0	1024	8000	8192	0.2	0.7	40	191.87
0.63	0	2048	8000	8192	0.3	0.7	40	460.11
0.63	0	4096	4560	16384	0.32	0.68	40	1156.2
0.63	0	8192	3193	32768	0.36	0.66	42	6183.85
0.63	0	16384	2432	32768	0.38	0.66	44	9954.44
0.64	0	128	24000	512	0.2	0.7	40	3.14
0.64	0	256	24000	1024	0.2	0.7	40	17.33
0.64	0	512	22400	2048	0.2	0.7	40	70.61
0.64	0	1024	11200	8192	0.2	0.7	40	305.41
0.64	0	2048	16000	8192	0.3	0.7	40	815.66
0.64	0	4096	12000	16384	0.32	0.68	40	3751.7
0.64	0	8192	3360	32768	0.36	0.66	42	6323.48
0.64	0	16384	2240	32768	0.38	0.66	44	9724.53
0.65	0	128	9600	512	0.3	0.7	40	1.96
0.65	0	256	9600	1024	0.3	0.7	40	7.83
0.65	0	512	9600	2048	0.3	0.7	40	32.98
0.65	0	1024	33600	4096	0.3	0.7	44	457.63
0.65	0	2048	33600	8192	0.3	0.7	40	2212.92
0.65	0	4096	19200	16384	0.32	0.68	40	6242.19
0.65	0	8192	15054	16384	0.36	0.66	42	14652.7
0.65	0	16384	10526	32768	0.38	0.66	44	42378.9
0.655	0	128	24000	512	0.2	0.7	40	3.05
0.655	0	256	24000	1024	0.2	0.7	40	14.69
0.655	0	512	16000	2048	0.2	0.7	40	43.48
0.655	0	1024	21920	4096	0.3	0.7	40	291.4
0.655	0	2048	20400	8192	0.3	0.7	40	1143.21
0.655	0	4096	18252	16384	0.32	0.68	40	6818.29
0.655	0	8192	12260	16384	0.36	0.66	42	11835.9
0.655	0	16384	5278	32768	0.38	0.66	44	22993.1
0.655	0	32768	3646	32768	0.38	0.66	44	29010.7

TABLE AII. Parameters of the simulations done at fixed temperature T and varying field h_r . $N(h_r)$ is the number of values of field taken in the range $h_r(\text{min,max})$. The equilibration times are different for different values of the field h_r , which lie in the range $N_{\text{sweep}}(\text{min,max})$. The number of disorder samples for different fields lie in the range $N_{\text{samp}}(\text{min,max})$. t_{tot} is the total CPU time consumed in hours to generate data for a particular system size.

σ	T	N	$h_r(\text{min,max})$	$N(h_r)$	$N_{\text{sweep}}(\text{min,max})$	$N_{\text{samp}}(\text{min,max})$	$t_{\text{tot}}(\text{hrs})$
0.6	0.38	128	(0.0100, 9.0000)	27	(1024, 1024)	(5000, 20000)	2.55
0.6	0.38	256	(0.0100, 9.0000)	27	(2048, 2048)	(5000, 30000)	18.5
0.6	0.38	512	(0.0100, 9.0000)	27	(2048, 2048)	(5000, 30000)	40.78
0.6	0.38	1024	(0.0100, 9.0000)	30	(4096, 4096)	(4000, 30000)	181.68
0.6	0.38	2048	(0.0100, 9.0000)	31	(4096, 8192)	(2500, 40000)	3506.91
0.6	0.38	4096	(0.0100, 9.0000)	31	(8192, 32768)	(4000, 75200)	9948.45
0.6	0.38	8192	(0.0100, 9.0000)	27	(16384, 262144)	(1200, 37050)	88881.3
0.6	0.38	16384	(0.0100, 9.0000)	29	(32768, 524288)	(240, 12749)	151254
0.6	0.38	32768	(0.1000, 0.1400)	3	(131072, 1048576)	(3813, 7596)	155371
0.63	0.364	128	(0.0100, 9.0000)	28	(512, 512)	(4000, 16000)	2.07
0.63	0.364	256	(0.0100, 9.0000)	33	(1024, 1024)	(4000, 32000)	16.06
0.63	0.364	512	(0.0100, 9.0000)	34	(2048, 2048)	(4000, 32000)	52.31
0.63	0.364	1024	(0.0100, 9.0000)	33	(4096, 4096)	(5000, 32000)	200.35
0.63	0.364	2048	(0.0100, 9.0000)	33	(4096, 8192)	(4000, 36000)	967.71
0.63	0.364	4096	(0.0100, 9.0000)	32	(8192, 32768)	(4000, 37440)	7357.41
0.63	0.364	8192	(0.0100, 9.0000)	33	(16384, 131072)	(643, 34251)	56078.5
0.63	0.364	16384	(0.0100, 9.0000)	30	(32768, 524288)	(640, 18941)	94942.1
0.63	0.364	32768	(0.0900, 0.1200)	4	(262144, 524288)	(4892, 14287)	159218
0.64	0.357	128	(0.0100, 9.0000)	27	(1024, 1024)	(5000, 40000)	4.56
0.64	0.357	256	(0.0100, 9.0000)	27	(2048, 2048)	(2000, 40000)	19.01
0.64	0.357	512	(0.0400, 9.0000)	25	(2048, 2048)	(2000, 50000)	48.42
0.64	0.357	1024	(0.0100, 9.0000)	28	(4096, 4096)	(2000, 40000)	190.31
0.64	0.357	2048	(0.0100, 9.0000)	28	(4096, 8192)	(1000, 40000)	791.55
0.64	0.357	4096	(0.0400, 9.0000)	25	(8192, 16384)	(1000, 36000)	4250.85
0.64	0.357	8192	(0.0100, 9.0000)	28	(16384, 131072)	(1600, 37120)	23608.4
0.64	0.357	16384	(0.0100, 9.0000)	28	(32768, 262144)	(320, 12800)	58060.3
0.65	0.35	128	(0.0100, 9.0000)	29	(1024, 1024)	(4000, 12000)	10.12
0.65	0.35	256	(0.0100, 9.0000)	29	(2048, 2048)	(4000, 12000)	14.64
0.65	0.35	512	(0.0100, 9.0000)	29	(4096, 4096)	(4000, 12000)	58.13
0.65	0.35	1024	(0.0100, 0.3000)	14	(8192, 8192)	(4000, 10000)	139.38
0.65	0.35	2048	(0.0100, 0.3000)	14	(16384, 16384)	(4800, 24000)	800.5
0.65	0.35	4096	(0.0100, 9.0000)	29	(32768, 32768)	(1200, 24000)	4786.42
0.65	0.35	8192	(0.0100, 0.3000)	14	(65536, 131072)	(800, 21551)	27908.2
0.65	0.35	16384	(0.0100, 0.3000)	14	(262144, 262144)	(551, 11602)	74407.7
0.655	0.344	128	(0.0100, 9.0000)	27	(1024, 1024)	(4000, 44000)	6.03
0.655	0.344	256	(0.0100, 9.0000)	29	(2048, 2048)	(4000, 44000)	30.18
0.655	0.344	512	(0.0100, 9.0000)	29	(4096, 4096)	(2000, 60000)	80.09
0.655	0.344	1024	(0.0100, 9.0000)	30	(8192, 8192)	(2000, 48000)	265.81
0.655	0.344	2048	(0.0100, 9.0000)	30	(16384, 16384)	(1000, 41600)	1838.4
0.655	0.344	4096	(0.0100, 9.0000)	29	(16384, 32768)	(960, 36960)	7440.49
0.655	0.344	8192	(0.0100, 9.0000)	32	(16384, 65536)	(480, 42800)	42173.3
0.655	0.344	16384	(0.0100, 9.0000)	32	(32768, 262144)	(576, 20479)	191977
0.655	0.344	32768	(0.0100, 9.0000)	29	(65536, 524288)	(256, 14707)	272176
0.655	0.344	65536	(0.0100, 0.2000)	8	(524288, 1048576)	(192, 3845)	245877